IEEE Access
Multidisciplinary | Rapid Review | Open Access Journal

Received 17 April 2023, accepted 3 May 2023, date of publication 10 May 2023, date of current version 25 May 2023.

Digital Object Identifier 10.1109/ACCESS.2023.3274773

RESEARCH ARTICLE

Optimized Nonlinear Integral Backstepping Controller for DC–DC Three-Level Boost Converters

IMANE AIT AYAD[1], ELMOSTAFA ELWARRAKI[1], SYED UMAID ALI[2], SAEED MIAN QAISAR[3,4], ASAD WAQAR[2], MOHAMED BAGHDADI[1], AND AHMAD ALZAHRANI[5]

[1]Laboratory of Electrical Systems, Energy Efficiency and Telecommunications, Faculty of Sciences and Technologies, Cadi Ayyad University, Marrakesh 40000, Morocco
[2]Center of Excellence in Artificial Intelligence (CoE-AI), Department of Electrical Engineering, Bahria University, Islamabad 44000, Pakistan
[3]Department of Electrical and Computer Engineering, Effat University, Jeddah 22332, Saudi Arabia
[4]LINEACT CESI, 69100 Lyon, France
[5]Electrical Engineering Department, College of Engineering, Najran University, Najran 11001, Saudi Arabia

Corresponding author: Asad Waqar (asadwaqar.buic@bahria.edu.pk)

This work was funded by the Deanship of Scientific Research at Najran University under the Research Groups Funding Program Grant code (NU/RG/SERC/12/7).

ABSTRACT Multi-level DC-DC converters have been widely used in automotive and other high-power applications. Thus, the control of these multi-level converters is an emerging thematic in power electronics to ensure their proper functioning. This paper provides a novel nonlinear control of a DC-DC three level boost converter (T-LBC) based on a backstepping (BS) technique with an integral action and is optimized using genetic algorithms (GA). Firstly, the average state model of the T-LBC is described. Then, this model is used to design an integral BS controller; nevertheless, the controller parameters are often determined manually, which may degrade the control quality. A genetic algorithm-based optimization method is applied to establish the best controller gains and improve the proposed controller efficiency. The asymptotic stability converter is verified using the Lyapunov method criteria. In order to validate the introduced controller under different scenarios, the Matlab/Simulink environment is used. In addition, it is compared with different controllers such as conventional backstepping, fuzzy logic, and proportional–integral–derivate (PID) controllers under varying references to highlight its performance further. Finally, the designed controller is verified experimentally by implementing it using a dSPACE 1104 control board. The simulation and experimental results show that the optimized integral BS controller presents the best performances in terms of settling time, overshoot and steady-state error.

INDEX TERMS Three level boost DC–DC converter, nonlinear control, integral backstepping, genetic algorithms, tuning.

I. INTRODUCTION

Nowadays, DC-DC multi-level converters are strongly recommended in several applications, such as renewable energy [1], [2], [3], [4], [5], [6], where medium- and high-power transmission are required, particularly a three-level boost DC-DC converter (T-LBC). Due to its topology, the T-LBC has the same high-voltage gain as the conventional boost but with lower inductor current ripples, reduced switching losses, and reduced volume [7]. Indeed, more and more applications use this architecture, especially in the automobile industry [8] and for power factor correction [9].

All DC-DC converters are nonlinear systems; the voltage gain varies nonlinearly with the duty cycle, so a control technique is required to achieve the DC bus voltage. The DC/DC

The associate editor coordinating the review of this manuscript and approving it for publication was Zhilei Yao.

converters control has always been an emerging research subject in electrical engineering that has experienced strong development.

Several authors have been handled the DC-DC converters control using different approaches to achieve the desired output converter voltage despite load or input variations. Thus, many controller types are used: conventional controllers, such as feedback and proportional–integral–derivative (PID); nonlinear ones, such as sliding mode and backstepping; and intelligent controllers, like fuzzy logic (FL) and particle swarm optimization (PSO).

In [10], a conventional controller based on feedback and PID has been used. Conventional controllers are easy to implement, but they are just suitable for linear systems and give slow response to disturbances [11]. A sliding mode controller for the voltage control of DC-DC buck-and-boost converters has been introduced in [12] and [13]. An adaptive PID controller has been presented in [14] and [15]. The nonlinear controllers are robust and suitable for nonlinear systems, but the main draw-back of sliding mode controllers is the oscillation phenomenon appearance called ''chattering'' [16]. This oscillation near the surface is not desirable, especially in DC-DC converters whose frequencies are very high. The adaptive PID controllers require significant computation time and ample memory space for data processing.

A fuzzy logic controller of a DC voltage control has been addressed in [17], [18], [19], and [20]. In [21], an optimized controller for a boost converter based on the PSO algorithm has been pro-posed. For the fuzzy logic technique, it is difficult to choose suitable membership functions, and it presents a high computational burden [16].

Thus, this study aims to present an optimized nonlinear controller based on an integral BS approach for the T-LBC. The BS controller is a robust control approach well suited to this nonlinear system. The BS controller has been widely described in the literature. Some BS controllers are briefly presented. In [22], the authors have proposed a maximum power point tracking (MPPT) controller based on a nonlinear BS controller with integral action. The results prove the integral BS controller superiority over other methods (perturb and observe (P&O) and FL). In [23], a BS controller has been developed for the specific suspension of the rotating impeller in the heart pump. The authors of [24] have proposed a new hybrid control method for induction motors based on the combination of the BS approach and the direct torque. The experimental results have shown that the optimized BS controller is more efficient than the traditional direct torque control compared to the literature results. In [25], a BS controller has been presented for a quadrotor. The control system demonstrates an excellent performance in the presence of parametric uncertainties. In [26], a fault-diagnosis control for the five phase induction motor based on a BS controller for ensuring the desired dynamic has been introduced. In [27], an integral backstepping controller for an inverter applied in an islanded micro-grid has been developed. A robust integral backstepping controller has been proposed for the energy management of Plugin hybrid electric vehicles [28], regarding the reference generation, voltage regulation, and smooth current tracking. In [29], an adaptive backstepping controller has been presented for a buck converter.

Thus, the BS controller is widely used in different applications, and the simulation and experimental results verify the robustness of this controller.

To design the BS controller, the state average system model is used. The performance of a BS controller is entirely dependent on the nonlinear system model, despite its efficiency and robustness. Real-world systems are susceptible to change over time; thus, the equations used to simulate them are also subject to change. Consequently, the BS controller's performance may degrade. This issue may be resolved with a simple update to the controller, including the integral action.

Summarizing the literature review for control of DC-DC converter, it can be stated:

- The control must ensure voltage regulation under sudden reference and load variations.
- The control must ensure high steady-state performances and quick dynamic response.
- A controller for DC- DC converter has to take into account the nonlinearity of the converter.
- BS technique for controller have been applied to incorporate the nonlinearity of the converter.
- With no standard for tuning the BS gains, some studies have indicated that the gains are manually tuned, while others have introduced automatic tuning via the fuzzy technique [30], [31].

This is why, in this study, we introduce a gains-tuning technique based on genetic algorithms (GA), which optimizes the BS controller for achieving the optimum converter response control tuning.

Therefore, this work aims to design a robust tuning integral BS controller using GA to find the most optimal control gains of a T-LBC. Fig. 1 illustrates the developed control scheme.

The paper contributions can be summarized as follows:

- A nonlinear integral backstepping control technique is proposed for the DC-DC T-LBC to overcome its nonlinearity (voltage gain varies nonlinearly with duty cycle).
- The proposed control technique performs optimization of the proposed controller using the GA to ensure quick dynamic response and high steady-state performances. Experimental validation of the proposed controller is performed using dSPACE 1104 control board.

The rest of the paper is presented as follows: part 2 presents T-LBC operation, part 3 describes the integral BS controller design based on the Lyapunov theory, and the tuning is performed using the GA in part 4. Parts 5 and 6 show the validation of the designed controller through the simulation and hardware results of the controller's response under different scenarios. In the end, the conclusions are presented in part 7.

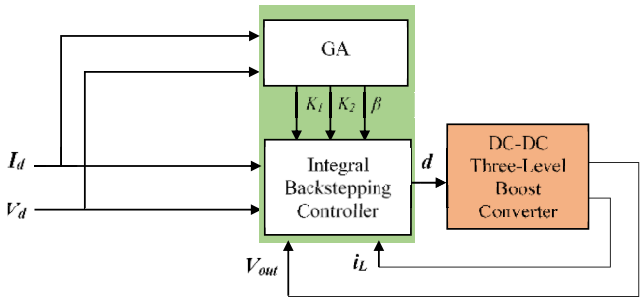

FIGURE 1. Diagram of the proposed control strategy.

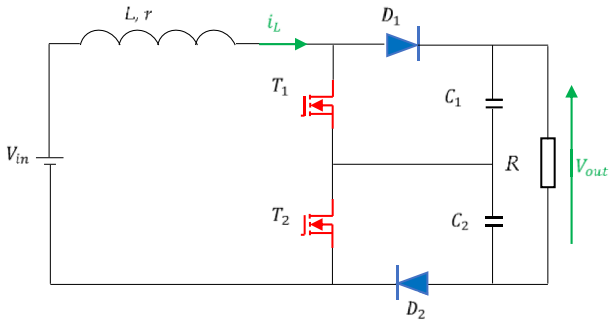

FIGURE 2. Three level boost converter.

II. THREE-LEVEL BOOST CONVERTER MATHEMATICAL MODELING

In this section, we present the operation principle of the DC-DC T-LBC. After that, we introduce the average model, covering all possible converter modes. The T-LBC is shown in Fig. 2. The T-LBC circuit consists of two power switches T_1 and T_2 (MOSFET), two fast recovery diodes D_1 and D_2, a DC input voltage V_{in}, an inductor L with an equivalent series resistor r, two output filter capacitors C_1 and C_2, and a resistor R as an output load. The power switches are controlled by the same duty cycle d and the same period T, but their PWM (pulse-width modulation) signals have a phase difference of 180°. Therefore, four switching modes are possible, as shown in Fig. 3. The circuit is supposed to be operated in continuous conduction mode with $C_1 = C_2$.

The output voltage is denoted V_{out}, the voltages across the output capacitors C_2 and C_1 are denoted V_{C1} and V_{C2}, and the current through the inductor is denoted i_L.

The switches control signals u_1 and u_2, inductor voltage V_L waveform, and the inductor current waveform i_L are shown in Fig. 4 for $d > 0.5$ and $d < 0.5$.

According to Fig. 3, there are four power states for the T-LBC operation. Only three states are involved in both cases $d > 0.5$ and $d < 0.5$; state 4 occurs when $d < 0.5$, and state 1 occurs when $d > 0.5$.

When $d < 0.5$ (Fig. 4(a)). From 0 to dT, the switch T_1 is closed and the switch T_2 is open (state 2), the current i_L increases, and the capacitor C_1 discharges, and capacitor C_2 is charged. From dT to T/2 and (d+ 0.5)T to T, the power switches T_1 and T_2 are open (state 4), the inductor current i_L decreases, C_1 and C_2 are all charged. From T/2 to ($d + 0.5$)T, T_1 is open and the switch T_2 is closed (switching state 3), the current in-creases, C_1 is charged, and the C_2 discharges.

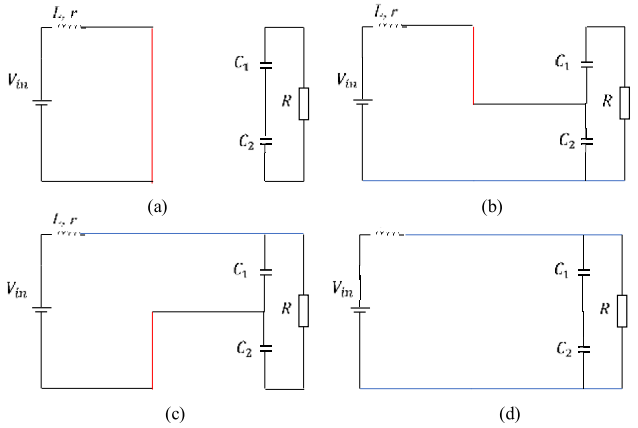

FIGURE 3. Normal operating modes in TLB converter. (a) State 1. (b) State 2. (c) State 3. (d) State 4.

When $d > 0.5$, as Fig. 4(b) shows, from 0 to (d-0.5)T and T/2 to dT, both the switches T_1 and T_2 are closed, the input current increases, and the output capacitors C_1 and C_2 discharge (state 1). From (d-0.5)T to T/2, the switch T_1 is closed and the switch T_2 is open (switching state 2), the energy stored in the inductor is transferred to output capacitor C_2, and the output capacitor C_1 discharges. From dT to T, T_1 is open and T_2 is closed (switching state 3), the input inductor current decreases, C_1 is charged, and C_2 discharges.

Each switching state is described by a differential equation, State 1 is presented by Equation 1:

$$\begin{cases} \dfrac{d}{dt} i_L = \dfrac{V_{in}}{L} \\ \dfrac{d}{dt} v_{C1} = -\dfrac{v_{C1} - v_{C2}}{RC_1} \\ \dfrac{d}{dt} v_{C2} = -\dfrac{v_{C1} - v_{C2}}{RC_2} \end{cases} \tag{1}$$

State 2 is presented by Equation 2:

$$\begin{cases} \dfrac{d}{dt} i_L = \dfrac{V_{in}}{L} - \dfrac{v_{C2}}{L} \\ \dfrac{d}{dt} v_{C1} = -\dfrac{v_{C1} - v_{C2}}{RC_1} \\ \dfrac{d}{dt} v_{C2} = \dfrac{i_L}{C_2} - \dfrac{v_{C1} - v_{C2}}{RC_2} \end{cases} \tag{2}$$

State 3 is described by Equation 3:

$$\begin{cases} \dfrac{d}{dt} i_L = \dfrac{V_{in}}{L} - \dfrac{v_{C1}}{L} \\ \dfrac{d}{dt} v_{C1} = \dfrac{i_L}{C_1} - \dfrac{v_{C1} - v_{C2}}{RC_1} \\ \dfrac{d}{dt} v_{C2} = -\dfrac{v_{C1} - v_{C2}}{RC_2} \end{cases} \tag{3}$$

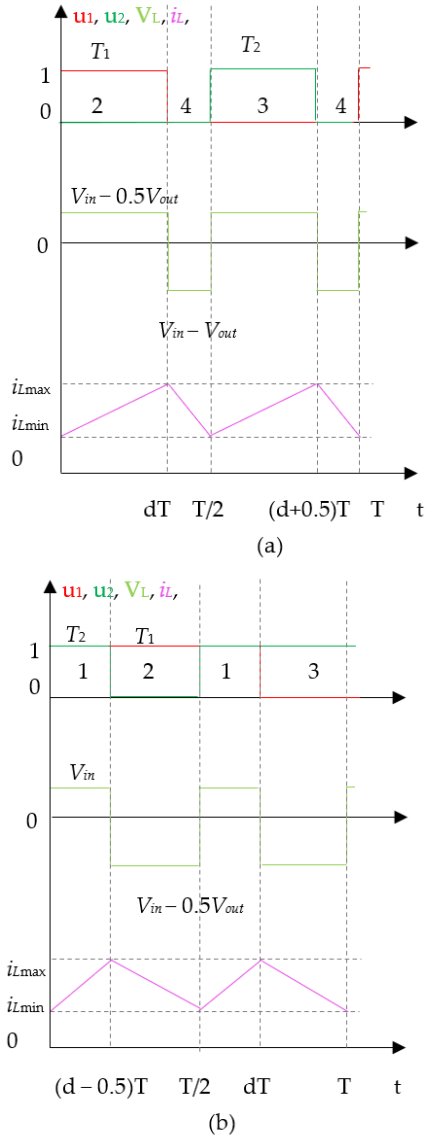

FIGURE 4. Waveforms of switches control signals, inductor voltage, and the inductor current. (a) For d < 0.5; (b) For d > 0.5.

State 4 is presented by Equation 4:

$$\begin{cases} \dfrac{d}{dt} i_L = \dfrac{V_{in}}{L} - \dfrac{v_{C1}}{L} - \dfrac{v_{C2}}{L} \\ \dfrac{d}{dt} v_{C1} = \dfrac{i_L}{C_1} - \dfrac{v_{C1} - v_{C2}}{RC_1} \\ \dfrac{d}{dt} v_{C2} = \dfrac{i_L}{C_2} - \dfrac{v_{C1} - v_{C2}}{RC_2} \end{cases} \tag{4}$$

By combining the previous differential equations, the average model of the T-LBC is given by:

$$\begin{cases} \dfrac{d}{dt} i_L = -(1-d)\dfrac{x_2}{L} + \dfrac{V_{in}}{L} \\ \dfrac{d}{dt} V_{out} = -2(1-d)\dfrac{x_1}{C} + \dfrac{2x_2}{RC} \end{cases} \tag{5}$$

Where $C = C_1 = C_2$ and $V_{out} = V_{C1} + V_{C2}$

The average mathematical model of the converter will be used to design the proposed controller in the next section.

III. PROPOSED CONTROLLER DESIGN

The new optimized integral BS controller is developed to ensure the output voltage control of the T-LBC converter. Firstly, the integral BS controller is designed based on the average mathematical model of the converter (Equation 5). Then, the control law is determined, so the tuning gain of the proposed controller is required. Therefore, the GA algorithm is used to find the suitable values of proposed controller gains.

The mathematical development of the integral BS and structure of the GA algorithm are explained below.

A. STEP 1: INTEGRAL BACKSTEPPING CONTROLLER DESIGN

Backstepping control is a systematic method for designing robust controller for a large class of nonlinear systems [33]. The backstepping expression refers to the recursive nature of its design procedure.

Since its appearance, this method has been applied to many fields of application. The basic idea is to transform the system, after a loop, into a set of nested subsystems, with "virtual" control laws defined for each subsystem. The control design procedure includes several steps. Initially, a subsystem is considered for which a virtual control law is constructed. Then, step by step, the system is extended until the actual command appears explicitly. At each step, a candidate Lyapunov function is designed to achieve the convergence of each of the subsystems. Using a method such as Lyapunov ensures the whole system is asymptotically stable.

In this approach, the controller objective is to force the output voltage to follow its reference by calculating a control law that will be applied to control the power switches of the converter. The BS technique application to T-LBC is based on 2 steps as the converter is of order 2.

Let $x_1 = i_L$ and $x_2 = V_{out}$, Equation (5) becomes:

$$\begin{cases} \dot{x}_1 = -(1-d)\dfrac{x_2}{L} + \dfrac{V_{in}}{L} \\ \dot{x}_2 = -2(1-d)\dfrac{x_1}{C} + \dfrac{2x_2}{RC} \end{cases} \tag{6}$$

Firstly, we define the inductor current error z_1:

$$z_1 = x_1 - I_d \tag{7}$$

where I_d is the reference current. The aim is to converge the error z_1 to zero.

Therefore,

$$\dot{z}_1 = \dot{x}_1 - \dot{I}_d = -(1-d)\frac{x_2}{L} + \frac{V_{in}}{L} - \dot{I}_d \tag{8}$$

Integral action is added into the error z_1 expression as given below:

$$e = z_1 + \Psi \tag{9}$$

where Ψ is given as:

$$\Psi = \int_0^t (x_1 - I_d)\, dt \tag{10}$$

Let us define Lyapunov candidate function as:

$$V_1 = \frac{1}{2} z_1^2 + \frac{\beta}{2} \Psi^2 \tag{11}$$

where β is a positive control gain, its time derivative is given by:

$$\dot{V}_1 = z_1 \dot{z}_1 + \beta \Psi \dot{\Psi} \tag{12}$$

Using (8) and derivative of (8), we obtain:

$$\dot{V}_1 = z_1 \left(- (1-d) \frac{x_2}{L} + \frac{V_{in}}{L} - \dot{I}_d + \beta \Psi \right) \tag{13}$$

To assure that the derivative of V_1 is negative, it is obligatory to choose:

$$-K_1 z_1 = - (1-d) \frac{x_2}{L} + \frac{V_{in}}{L} - \dot{I}_d + \beta \Psi \tag{14}$$

where K_1 is a positive gain, rewriting (14) as:

$$\frac{x_2}{L} = \frac{1}{(1-d)} \left(\frac{V_{in}}{L} - \dot{I}_d + K_1 z_1 + \beta \Psi \right) \tag{15}$$

Equation (15) will be the reference output voltage, given by:

$$\gamma_1 = \frac{1}{(1-d)} \left(\frac{V_{in}}{L} - \dot{I}_d + K_1 z_1 + \beta \Psi \right) \tag{16}$$

γ_1 presents the stabilization function.

Hence, let us define the second error:

$$z_2 = \frac{x_2}{L} - \gamma_1 \tag{17}$$

Rewriting (17):

$$\frac{x_2}{L} = z_2 + \gamma_1 \tag{18}$$

Replacing (18) in (8) gives:

$$\dot{z}_1 = -K_1 z_1 - (1-d) z_2 - \beta \Psi \tag{19}$$

Let us examine the derivation of z_2:

$$\dot{z}_2 = 2(1-d) \frac{x_1}{LC} - 2 \frac{x_2}{RLC} - \dot{\gamma}_1 \tag{20}$$

$$\dot{\gamma}_1 = \frac{1}{(1-d)} \left(\dot{d} \gamma_1 - \ddot{I}_d - K_1^2 z_1 - K_1 z_2 (1-d) - K_1 \beta \Psi + \beta \dot{\Psi} \right) \tag{21}$$

Inserting $\dot{\gamma}_1$ from (21) in (20) $\dot{z}_2$becomes:

$$\dot{z}_2 = \frac{2(1-d) x_1}{LC} - \frac{2x_2}{LRC} - \frac{\gamma_1 \dot{d}}{1-d} + \frac{K_1^2 z_1 + (1-d) K_1 z_2 + \ddot{I}_d + K_{1\beta\Psi} - \beta \dot{\Psi}}{1-d} \tag{22}$$

Now, to ensure convergence of both z_1 and z_2 to zero, a second Lyapunov function V_2 is used whose time derivative must be negative.

$$V_2 = V_1 + \frac{1}{2} z_2^2 \tag{23}$$

TABLE 1. GA parameter.

Parameter	Value
Population size	30
Generations	10
Mutation probability	10%
Selection method	Rank selection
Crossover type	Heuristic

Its time derivative is given by:

$$\dot{V}_2 = \dot{V}_1 + z_2 \dot{z}_2 \tag{24}$$

$$V_2 = -K_1 z_1^2 - K_2 z_2^2 + z_2 \left[K_2 z_2 - (1-d) z_1 + \dot{z}_2 \right] \tag{25}$$

where K_2 is a positive gain, to ensure that V_2 is negative, it is obligatory:

$$-z_1 (1-d) + \dot{z}_2 + K_2 z_2 = 0 \tag{26}$$

Developing (26), the control law is given by:

$$\dot{d} = \frac{1}{\gamma_1} \left(\frac{2(1-d)^2 x_1}{LC} - \frac{2(1-d) x_2}{RLC} + \beta K_1 \Psi + \ddot{I}_d + z_1 \left[-(1-d)^2 + K_1^2 - \beta \right] + z_2 \left[(K_1 + K_2)(1-d) \right] \right) \tag{27}$$

We can see that when the equilibrium is achieved:

$$z_1 = z_2 \to 0; x_1 \to I_d; x_2 \to \frac{V_{in}}{1-d},$$

Equation (27) is reduced to:

$$\dot{d} = \frac{2(1-d)}{RCV_{in}} \left[(1-d)^2 R I_d - V_{in} \right]$$

$$f(i_L, V_{out}) = \sqrt{\frac{1}{2} [(i_L(t) - I_d(t))^2 + (V_{out}(t) - V_d(t))]^2} \tag{28}$$

If $\dot{d} = 0$, so $d_1 = 1 - \sqrt{\frac{V_{in}}{RI_d}}$; $d_2 = 1 + \sqrt{\frac{V_{in}}{RI_d}}$ and $d_3 = 1$.

The solution d_1 has a physical signification $0 < d_1 < 1$. On the other hand, if we plot the curve $d = f(d)$ expressed in equation III.28, we find that the equilibrium point d_1 is asymptotically stable. Thus, in $d_1$the neighborhood, Equation (28) becomes:

$$\dot{d} = \frac{4(d_2 - d)}{RC} \tag{29}$$

To conclude, the control law:

$$\dot{d} = \frac{1}{\gamma_1} \left(\frac{2(1-d)^2 x_1}{LC} - \frac{2(1-d) x_2}{RLC} + \beta K_1 \Psi + \ddot{I}_d + z_1 \left[-(1-d)^2 + K_1^2 - \beta \right] + z_2 \left[(K_1 + K_2)(1-d) \right] \right)$$

asymptotically stabilizes the system around the equilibrium point $(I_d, V_d, d = 1 - \sqrt{\frac{V_{in}}{RI_d}} = 1 - \frac{V_{in}}{V_d}$, where V_d is the

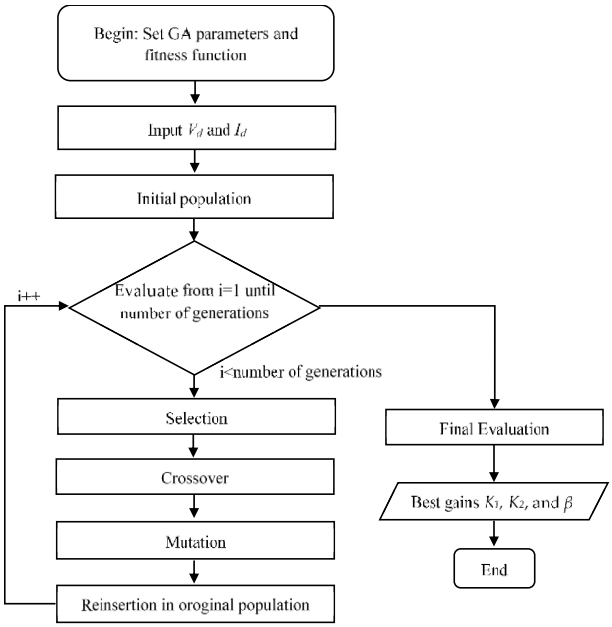

FIGURE 5. Flowchart of the GA used.

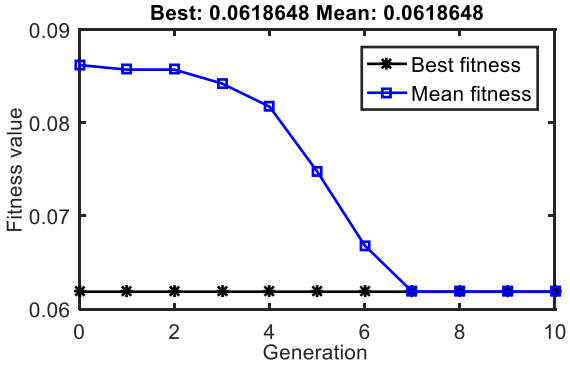

FIGURE 6. Fitness function convergence.

desired output voltage and:

$$\begin{cases} z_1 = x_1 - I_d \\ z_2 = \dfrac{x_2}{L} - \gamma_1 \\ \gamma_1 = \dfrac{1}{(1-d)}\left(\dfrac{V_{in}}{L} - \dot{I}_d + K_1 z_1 + \beta\Psi\right) \\ I_d = \dfrac{V_d^2}{RV_{in}} \end{cases}$$

The gains K_1, K_2, and β are the only parameters that remain unknown so tuning of the proposed controller is required.

B. STEP 2: TUNING THE INTEGRAL BS CONTROLLER GAINS USING GENETIC ALGORITHMS

GA use three main genetic operators: selection, crossover, and mutation [34]. First, possible solutions are selected to construct the initial population. Then, the better suited solutions are selected according to predefined reliability criteria. Once the fittest solutions are chosen, a crossover operator combines these solutions to produce a new population. The mutation operator guarantees the search-space exploration of the optimal solution.

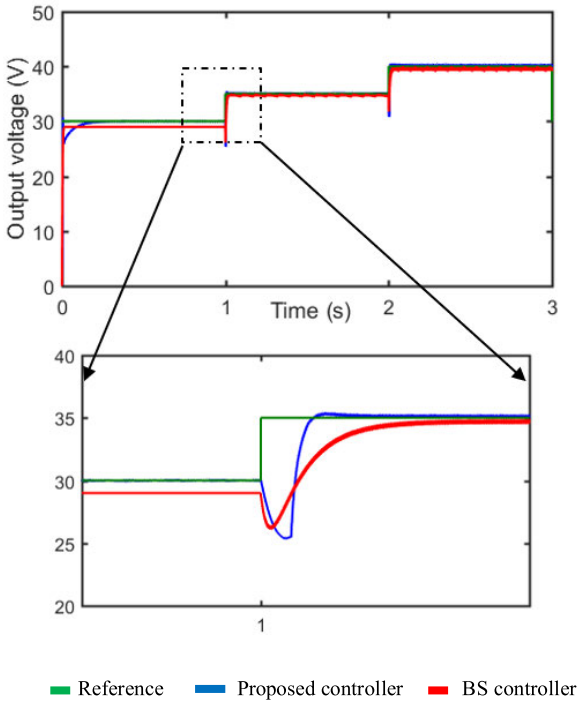

FIGURE 7. Output voltage responses under reference tracking.

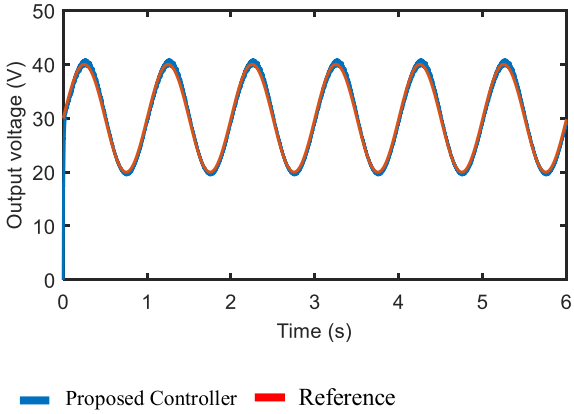

FIGURE 8. Output voltage comparison under varying reference.

TABLE 2. T-LBC and controller parameters.

Parameter	Value
C_2, C_1	700 µF
R	30 Ω
L	10 mH
R	0.25 mΩ
f	32 kHz
K_1	1.692×10^4
K_2	2.902×10^5
B	3.302×10^5

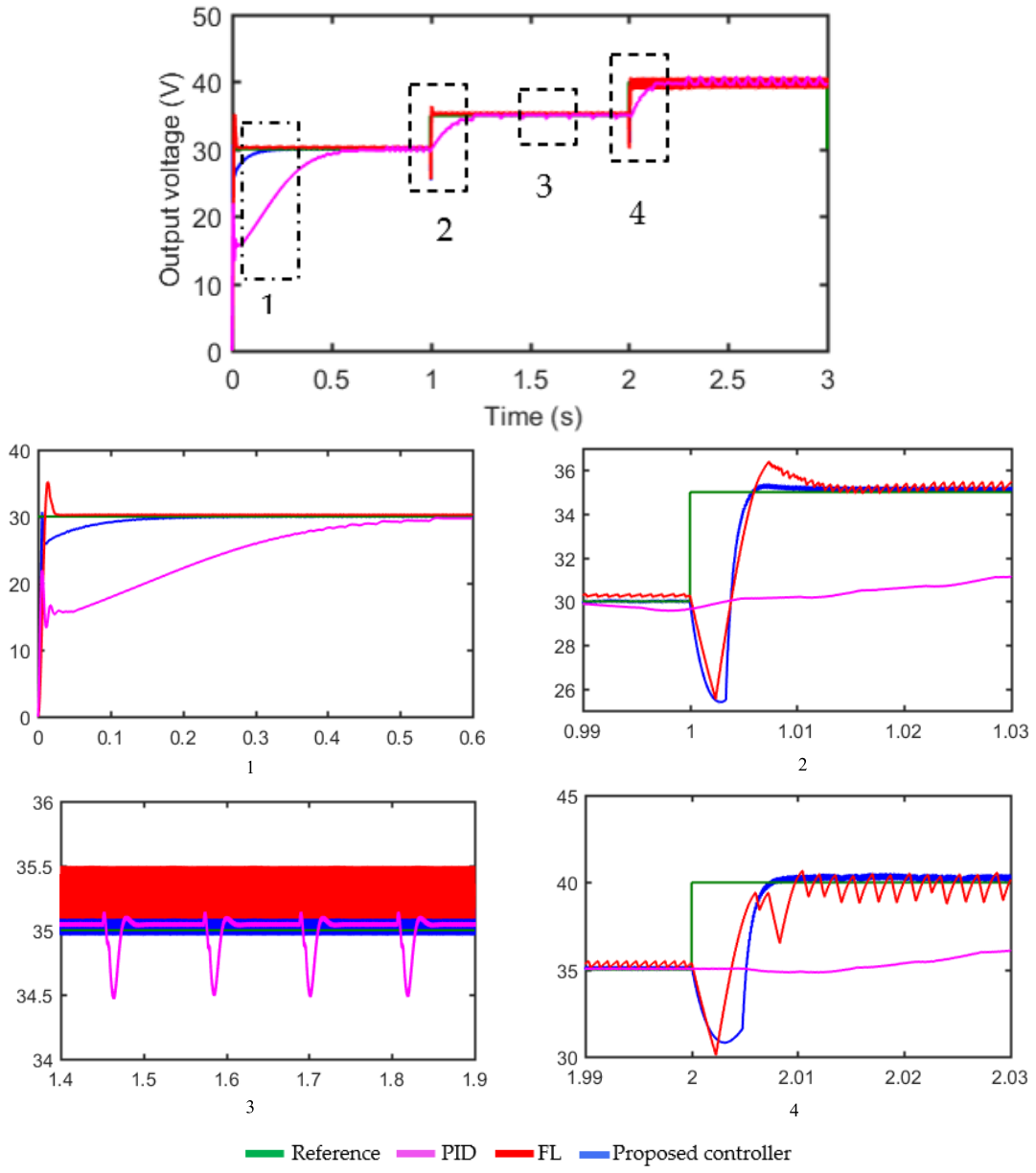

FIGURE 9. Output voltage comparison under varying reference.

TABLE 3. Comparison of time domain specifications of the proposed controller with PID, FL and conventional BS.

Controllers	Settling time (ms)			Overshoot (%)			Steady-state error (%)			Oscillations
	30 V	35 V	40 V	30 V	35 V	40 V	30 V	35 V	40 V	
PID	540	201	350	10	0.5	5	2.5	2.5	8	High
Fuzzy logic	35	13	12	14.5	5	0.5	1.5	1.5	5	Moderate
Conventional BS	50	10.5	11	0	0	0	6.6	1.2	2.5	Low
Proposed controller	45	4.5	5	0	0.25	0	0.1	0.5	1.25	Low

The aim of using GA is to find the optimal gains K_1, K_2, and β of the established controller in part A to guarantee the system stability by ensuring Lyapunov function negativity and suitable time response. The flowchart of the GA used is given in Fig. 5 and Table 1 lists the GA parameters.

The fitness function used to search the suitable gains K_1, K_2, and β of the proposed controller is chosen to be the

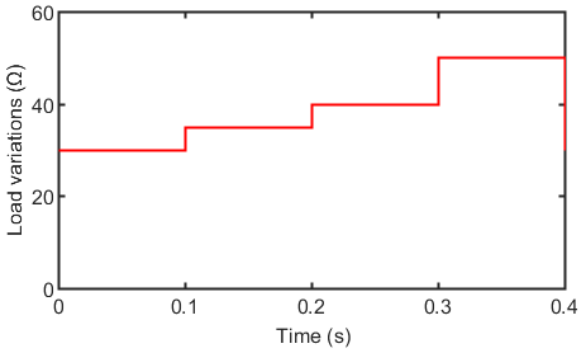

FIGURE 10. Load variations.

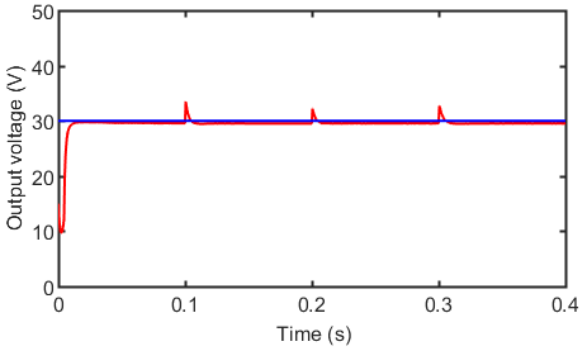

FIGURE 11. Output voltage response under varying load.

root integral mean square error expressed by Equations (30) and (31). Fig. 6 presents fitness function convergence characteristics.

$$f\ (x_1, x_2) = \sqrt{\frac{1}{2}\sum_{i=1}^{2}(x_i\ (t) - x_{di}(t))^2} \tag{30}$$

$$f\ (i_L, V_{out}) = \sqrt{\frac{1}{2}[(i_L(t) - I_d(t))^2 + (V_{out}(t) - V_d(t))]^2} \tag{31}$$

IV. SIMULATIONS AND RESULTS

A. COMPARISON OF THE PROPOSED CONTROLLER WITH THE CONVENTIONAL BS ONE

To validate the optimized integral BS controller performance, Matlab/ Simulink simulations are deployed. Table 2 lists the controller gain and the converter parameters. The simulation results are divided into two parts. In the first scenario, the designed controller performances under the variable steps in the reference voltage are analyzed. In the second scenario, the reference voltage tracking is used. The designed controller is compared to the conventional BS.

In the first scenario, the proposed controller is simulated for the variable step [30 V, 35 V (at t = 1 s), 40 V (at t = 2 s)].

According to Fig. 7, we can see that the output voltage controlled by the integral tuning BS using the GA perfectly follows the reference from one step to another one, with good precision and stability, compared to the conventional BS controller in terms of settling time and steady-state error.

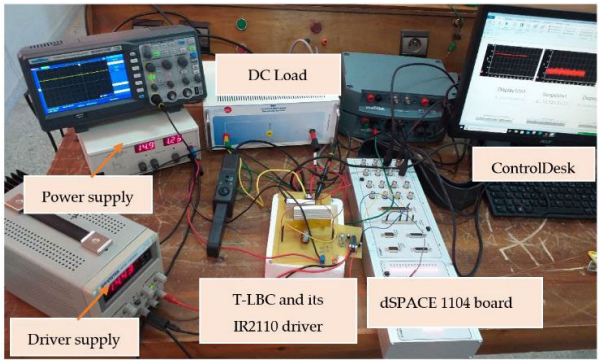

FIGURE 12. Experimental setup.

In the second scenario, the proposed controller is simulated for a reference voltage tracking, and the reference expression is given by $V_d = 30 + 10 \sin(2\ p\ 0.5\ t)$.

Fig. 8 presents the output converter voltage response of the proposed controller. It can be seen that the output voltage perfectly follows the desired value with a high performance.

B. COMPARISON OF THE PROPOSED CONTROLLER WITH FUZZY LOGIC AND PID CONTROLLERS

This section illustrates a comparison of the optimized integral BS controller with the FL and PID controllers to show the BS technique efficiency. The established results under varying reference [30 V, 35 V (at t = 1 s), 40 V (at t = 2 s)] are illustrated in Fig. 9.

According to Fig. 9 and Table 3 , the PID controller presents the lowest performance and its dynamic response is characterized by significant oscillations, important settling time ($\approx$ 201 ms) and steady-state error (it can attain 8 %) which disturb the correct operation of the system. The FL suitably follows the change in reference but with an important overshoot ($\approx$ 14.5 %) and significant oscillations around the desired voltage value. The proposed controller is able to correctly track the reference and its dynamic and static performance is better than that of PID and FL in terms of the steady-state error ($\approx$ 1.25 %), the settling time ($\approx$ 5 ms), the overshot ($\approx$ 0 %) and the oscillations in the static regime.

The simulation results verify the proposed controller's robustness and flexibility over the conventional BS, fuzzy logic, and PID controllers. The settling time, overshoot, steady-state error and oscillations are reduced.

C. LOAD VARIATIONS

In order to see the behaviour of the optimized integral BS controller under load variations, a simulation is conducted under a sudden variation in the load step [30 Ω, 35 Ω (at t = 0.1 s), 40 Ω (at t = 0.2 s), 50 Ω (at t = 0.3 s)].

Fig. 10 illustrates the load variations and Fig. 11 presents the output voltage response. The proposed controller keeps providing the suitable duty cycle for each load value. Then, the voltage keeps perfectly following the reference voltage.

V. EXPERIMENTAL RESULTS

This section presents the experimental tests to validate our laboratory's proposed controller for the T-LBC realized. The

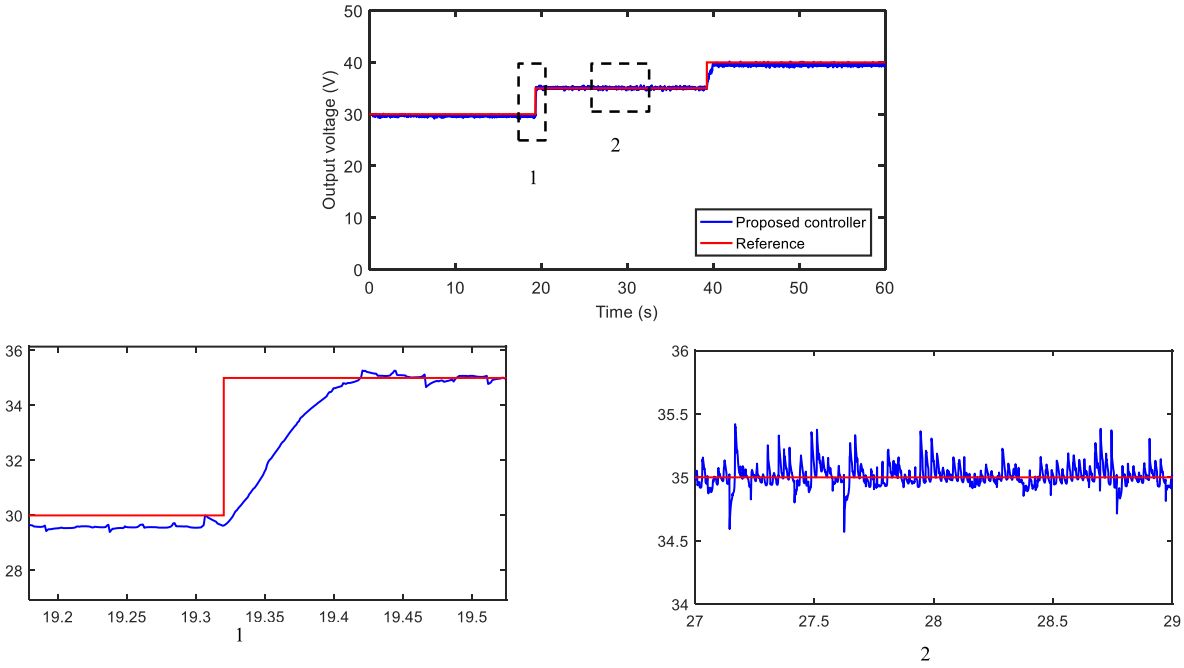

FIGURE 13. Experimental results of the proposed controller under varying reference: output voltage response.

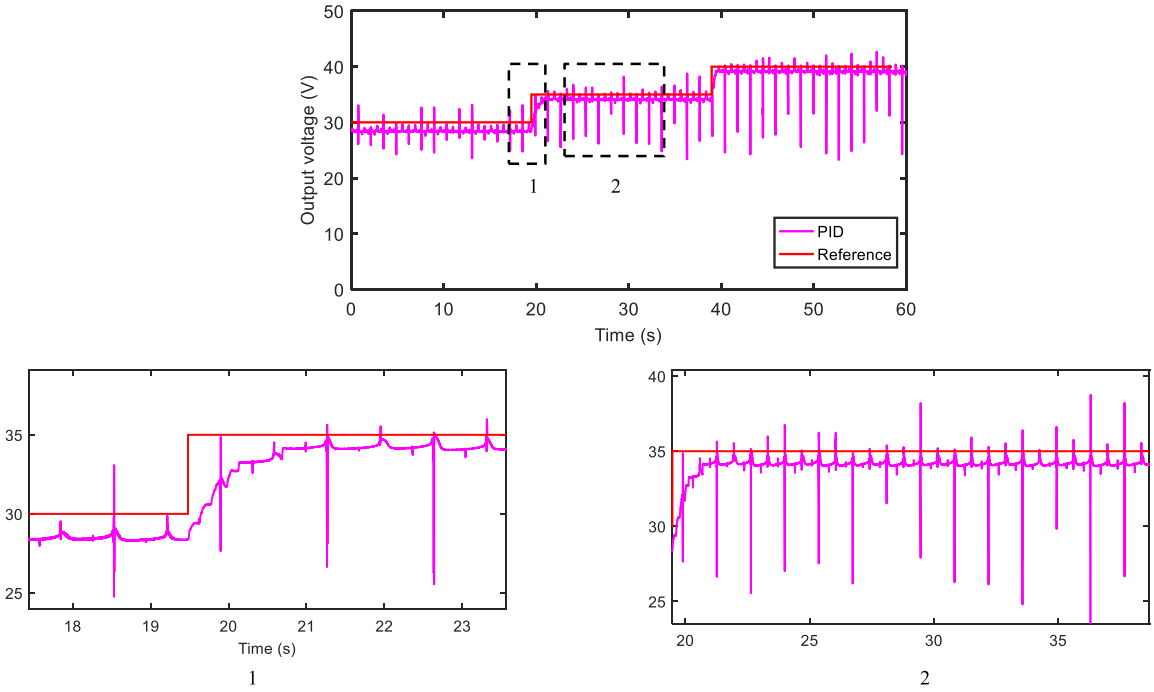

FIGURE 14. Experimental results of the PID controller: output voltage response.

experimental bench is illustrated in Fig. 12. The power part comprises a T-LBC, DC input source, and resistive load. For Mosfet's converter, IRFP460A devices are used. An IR2110 driver controls them.

The command part comprises the IR2110 driver to control the power switches' circuit and the dSPACE DS1104 controller board implemented in a real-time interface (RTI) and tests the proposed controller designed in Matlab/Simulink. The interface dSPACE Control Desk is used to visualize the output voltage in real time.

A variable step is used as a voltage reference. Then, the output voltage behavior of the converter is evaluated. Fig. 13, Fig. 14, Fig. 15 and Fig.16 present the experimental results.

According to Fig. 13, the measured voltage follows the reference variation with a low steady error (1.5%) and a low settling time ($t_s \approx 100$ ms).

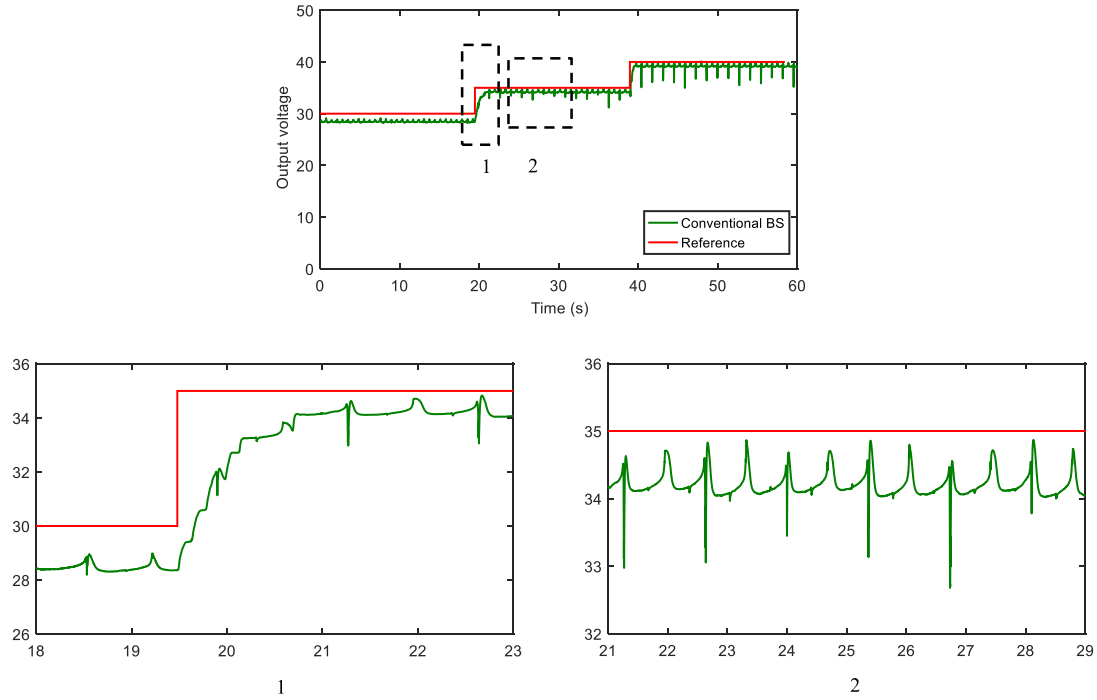

FIGURE 15. Experimental results of the BS conventional: output voltage response.

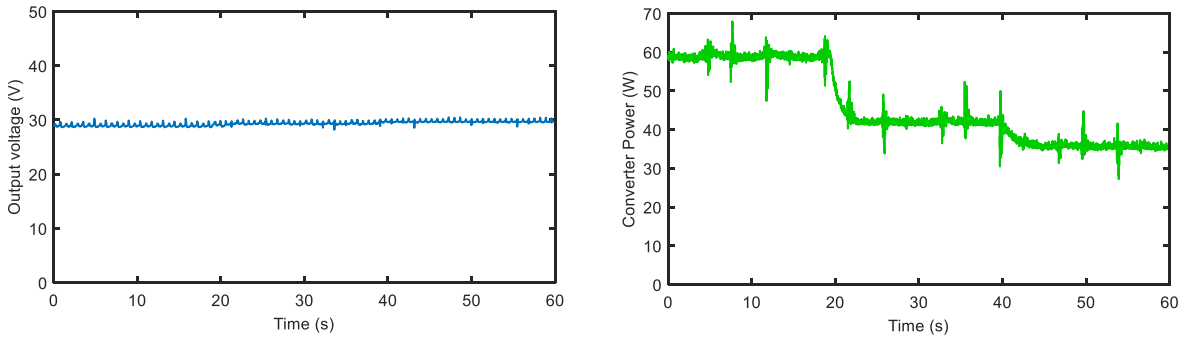

FIGURE 16. Experimental results of the proposed controller under varying load: (a) Output voltage; (b) Converter power.

TABLE 4. Experimental comparison of time domain specifications of the proposed controller with PID and conventional BS controller.

Controllers	Average Settling Time (s)	Average Steady-state Error (%)	Oscillations
PID	1	3.8	High
Conventional BS	0.79	3.1	Moderate
Proposed controller	0.1	1.5	Low

To validate the effectiveness of the proposed controller experimentally, Fig. 14 illustrates the results of the PID controller, the output voltage presents important oscillations and a steady-state error can reach 3.8 %. Fig. 15 illustrates the output voltage response of the BS controller.

It can be seen that the proposed controller presents a low settling time, low oscillations and a low steady-state error compared to the PID and BS conventional controllers as shown in Table 4. Thus, the experimental and simulation results validate the optimized integral BS controller that ensures the converter voltage regulation with good performance.

Fig. 16 presents the experimental results of the proposed controller under varying load. Fig. 16(b) presents the converter power to show the load variation. Fig. 16(a) presents the output voltage response, it can be seen that the converter voltage keeps the same value with the load variation.

The internet of energy (IoE) and cloud computing will be the crucial aspects in future smart grids. The event-driven tools will be more favorable in this situation in terms of real-time compression and decreased power consumption overhead [35]. Moreover, the performance of the recommended approach can be improved by including alternative optimization techniques [36]. Further investigation can be

conducted to see whether it is feasible to use these tools with the suggested technique.

VI. CONCLUSION

This paper aims to introduce a novel integral tuning backstepping controller using GA to control a DC-DC T-LBC with high precision and stability. Using the state average model of the T-LBC, the proposed controller was designed in two steps using the stability Lyapunov function in order to develop the law control of the T-LBC. In addition, a GA was used to find the suitable gain of the proposed controller. Firstly, the proposed controller was verified in simulation using Matlab/Simulink under several scenarios. Then, it was compared to the conventional BS, PID, and FL controllers. Finally, the designed controller was validated experimentally using a dSPACE 1104 board. The simulation and hardware results demonstrated that the proposed controller rapidly detected the reference variations with a very high performance, contrary to the other controllers.

ACKNOWLEDGMENT

The authors are grateful to the Cadi Ayyad University, Bahria University, Effat University, LINEACT CESI, and Najran University for the technical support.

REFERENCES

[1] A. Iqbal, A. Waqar, R. Madurai Elavarasan, M. Premkumar, T. Ahmed, U. Subramaniam, and S. Mekhilef, "Stability assessment and performance analysis of new controller for power quality conditioning in microgrids," *Int. Trans. Electr. Energy Syst.*, vol. 31, no. 6, Jun. 2021, Art. no. e12891.

[2] S. U. Ali, A. Waqar, M. Aamir, S. M. Qaisar, and J. Iqbal, "Model predictive control of consensus-based energy management system for DC microgrid," *PLoS ONE*, vol. 18, no. 1, Jan. 2023, Art. no. e0278110.

[3] I. A. Ayad, E. Elwarraki, and M. Baghdadi, "MPPT comparison of standalone photovoltaic system using multi-level boost converter," in *Proc. 4th Global Power, Energy Commun. Conf. (GPECOM)*, Jun. 2022, pp. 395–399, doi: 10.1109/GPECOM55404.2022.9815738.

[4] F. Haroon, M. Aamir, A. Waqar, S. Mian Qaisar, S. U. Ali, and A. T. Almaktoom, "A composite exponential reaching law based SMC with rotating sliding surface selection mechanism for two level three phase VSI in vehicle to load applications," *Energies*, vol. 16, no. 1, p. 346, Dec. 2022.

[5] M. S. Ali, S. U. Ali, S. M. Qaisar, A. Waqar, F. Haroon, and A. Alzahrani, "Techno-economic analysis of hybrid renewable energy-based electricity supply to gwadar, Pakistan," *Sustainability*, vol. 14, no. 23, p. 16281, Dec. 2022.

[6] T. Ahmed, A. Waqar, R. M. Elavarasan, J. Imtiaz, M. Premkumar, and U. Subramaniam, "Analysis of fractional order sliding mode control in a D-STATCOM integrated power distribution system," *IEEE Access*, vol. 9, pp. 70337–70352, 2021.

[7] I. Ait Ayad, E. Elwarraki, and M. Baghdadi, "Intelligent perturb and observe based MPPT approach using multilevel DC–DC converter to improve PV production system," *J. Electr. Comput. Eng.*, vol. 2021, pp. 1–13, Feb. 2021.

[8] T. Ahmed, A. Waqar, E. A. Al-Ammar, W. Ko, Y. Kim, M. Aamir, and H. U. R. Habib, "Energy management of a battery storage and D-STATCOM integrated power system using the fractional order sliding mode control," *CSEE J. Power Energy Syst.*, vol. 7, no. 5, pp. 996–1010, 2020.

[9] M. Lee and J.-S. Lai, "Fixed-frequency hybrid conduction mode control for three-level boost PFC converter," *IEEE Trans. Power Electron.*, vol. 36, no. 7, pp. 8334–8346, Jul. 2021, doi: 10.1109/TPEL.2020.3042157.

[10] R. Krishna, D. E. Soman, S. K. Kottayil, and M. Leijon, "Pulse delay control for capacitor voltage balancing in a three-level boost neutral point clamped inverter," *IET Power Electron.*, vol. 8, no. 2, pp. 268–277, Feb. 2015.

[11] S. U. Ali, M. Aamir, A. R. Jafri, U. Subramaniam, F. Haroon, A. Waqar, and M. Yaseen, "Model predictive control—Based distributed control algorithm for bidirectional interlinking converter in hybrid microgrids," *Int. Trans. Elect. Energy Syst.*, vol. 31, no. 10, Oct. 2021, Art. no. e12817.

[12] J. Zhang, D. G. Dorrell, L. Li, and A. Argha, "A novel sliding mode controller for DC–DC boost converters under input/load variations," in *Proc. 41st Annu. Conf. IEEE Ind. Electron. Soc.*, Nov. 2015, pp. 001698–001703, doi: 10.1109/IECON.2015.7392346.

[13] S. B. Hamed, M. B. Hamed, and L. Sbita, "Robust voltage control of a buck DC–DC converter: A sliding mode approach," *Energies*, vol. 15, no. 17, p. 6128, Aug. 2022, doi: 10.3390/en15176128.

[14] H. Li, X. Liu, and J. Lu, "Research on linear active disturbance rejection control in DC/DC boost converter," *Electronics*, vol. 8, no. 11, p. 1249, Oct. 2019.

[15] A. G. Soriano-Sánchez, M. A. Rodríguez-Licea, F. J. Pérez-Pinal, and J. A. Vázquez-López, "Fractional-order approximation and synthesis of a PID controller for a buck converter," *Energies*, vol. 13, no. 3, p. 629, Feb. 2020.

[16] F. Mumtaz, N. Zaihar Yahaya, S. Tanzim Meraj, B. Singh, R. Kannan, and O. Ibrahim, "Review on non-isolated DC–DC converters and their control techniques for renewable energy applications," *Ain Shams Eng. J.*, vol. 12, no. 4, pp. 3747–3763, Dec. 2021.

[17] I. A. Ayad and E. Elwarraki, "Output voltage control analysis of three-level boost DC–DC converters," in *Proc. 4th World Conf. Complex Syst. (WCCS)*, 2019, pp. 1–6, doi: 10.1109/ICoCS.2019.8930757.

[18] I. A. Ayad, E. E. Warraki, and A. Nouri, "A self-tuning fuzzy PI controller for three-level boost converter," in *Proc. 6th Int. Renewable Sustainable Energy Conf. (IRSEC)*, 2018, pp. 1–6, doi: 10.1109/IRSEC.2018.8702931.

[19] H. Farsizadeh, M. Gheisarnejad, M. Mosayebi, M. Rafiei, and M. H. Khooban, "An intelligent and fast controller for DC/DC converter feeding CPL in a DC microgrid," *IEEE Trans. Circuits Syst. II, Exp. Briefs*, vol. 67, no. 6, pp. 1104–1108, Jun. 2020, doi: 10.1109/TCSII.2019.2928814.

[20] P. Hema Rani, S. Navasree, S. George, and S. Ashok, "Fuzzy logic supervisory controller for multi-input non-isolated DC to DC converter connected to DC grid," *Int. J. Electr. Power Energy Syst.*, vol. 112, pp. 49–60, Nov. 2019.

[21] M. Arsalan, R. Iftikhar, I. Ahmad, A. Hasan, K. Sabahat, and A. Javeria, "MPPT for photovoltaic system using nonlinear backstepping controller with integral action," *Sol. Energy*, vol. 170, pp. 192–200, Aug. 2018.

[22] A. J. Humaidi, S. K. Kadhim, and A. S. Gataa, "Development of a novel optimal backstepping control algorithm of magnetic impeller-bearing system for artificial heart ventricle pump," *Cybern. Syst.*, vol. 51, no. 4, pp. 521–541, May 2020.

[23] S. Chaouch, L. Abdou, L. C. Alaoui, and S. Drid, "Optimized torque control via backstepping using genetic algorithm of induction motor," *Automatika*, vol. 57, no. 2, pp. 379–386, Jan. 2016.

[24] O. Rodríguez-Abreo, J. M. Garcia-Guendulain, R. Hernández-Alvarado, A. F. Rangel, and C. Fuentes-Silva, "Genetic algorithm-based tuning of backstepping controller for a quadrotor-type unmanned aerial vehicle," *Electronics*, vol. 9, no. 10, p. 1735, Oct. 2020.

[25] P. Vu, Q. Nguyen, M. Tran, G. Todeschini, and S. Santoso, "Adaptive backstepping approach for DC-side controllers of Z-source inverters in grid-tied PV system applications," *IET Power Electron.*, vol. 11, no. 14, pp. 2346–2354, Nov. 2018.

[26] M. A. Mossa and H. Echeikh, "A novel fault tolerant control approach based on backstepping controller for a five phase induction motor drive: Experimental investigation," *ISA Trans.*, vol. 112, pp. 373–385, Jun. 2021.

[27] A. A. Shah, X. Han, H. Armghan, and A. A. Almani, "A nonlinear integral backstepping controller to regulate the voltage and frequency of an islanded microgrid inverter," *Electronics*, vol. 10, no. 6, p. 660, Mar. 2021.

[28] Z. E. Huma, M. K. Azeem, I. Ahmad, H. Armghan, S. Ahmed, and H. M. M. Adil, "Robust integral backstepping controller for energy management in plugin hybrid electric vehicles," *J. Energy Storage*, vol. 42, Oct. 2021, Art. no. 103079.

[29] S. A. Saadat, S. M. Ghamari, and H. Mollaee, "Adaptive backstepping controller design on buck converter with a novel improved identification method," *IET Control Theory Appl.*, vol. 16, no. 5, pp. 485–495, Mar. 2022, doi: 10.1049/cth2.12241.

[30] F. Massaoudi, D. Elleuch, and T. Damak, "Robust control for a two DOF robot manipulator," *J. Electr. Comput. Eng.*, vol. 2019, Apr. 2019, Art. no. 391986.

[31] S. Huang, J. Huang, Z. Cai, and H. Cui, "Adaptive backstepping sliding mode control for quadrotor UAV," *Sci. Program.*, 2021, Art. no. 3997648.
[32] W. Kong, D. Zhou, Z. Yang, Y. Zhao, and K. Zhang, "UAV autonomous aerial combat maneuver strategy generation with observation error based on state-adversarial deep deterministic policy gradient and inverse reinforcement learning," *Electronics*, vol. 9, no. 7, p. 1121, Jul. 2020.
[33] P. S. Prakash, R. Kalpana, B. Singh, and G. Bhuvaneswari, "Power quality improvement in utility interactive based AC–DC converter using harmonic current injection technique," *IEEE Trans. Ind. Appl.*, vol. 54, no. 5, pp. 5355–5366, Sep. 2018, doi: 10.1109/TIA.2018.2855142.
[34] M. Baghdadi, E. Elwarraki, N. Mijlad, and I. A. Ayad, "SIMSCAPE electrical modelling of the IGBT with parameter optimization using genetic algorithm," *J. Electr. Comput. Eng.*, vol. 2021, pp. 1–11, May 2021.
[35] S. Mian Qaisar and F. Alsharif, "Signal piloted processing of the smart meter data for effective appliances recognition," *J. Electr. Eng. Technol.*, vol. 15, no. 5, pp. 2279–2285, Sep. 2020.
[36] H. Khan, I. F. Nizami, S. M. Qaisar, A. Waqar, M. Krichen, and A. T. Almaktoom, "Analyzing optimal battery sizing in microgrids based on the feature selection and machine learning approaches," *Energies*, vol. 15, no. 21, p. 7865, Oct. 2022.

IMANE AIT AYAD was born in Marrakesh, Morocco, in 1994. She received the B.S. degree in industrial informatics, electronics and automatic from the Faculty of Sciences and Technologies, Cadi Ayyad University, Marrakesh, in 2015, and the M.S. degree in electrical engineering from Cadi Ayyad University, in 2017, where she is currently pursuing the Ph.D. degree in electrical engineering and energy efficiency with the Electrical Systems, Energy Efficiency and Telecommunications Laboratory.

Her research interests include power electronics, the control of dc–dc power converters, fault diagnosis, renewable energies, artificial intelligence, and control nonlinearities.

ELMOSTAFA ELWARRAKI received the master's degree, in 1996, the Ph.D. degree in electrical engineering, in 2001, and the Ph.D. degree in information processing, in 2007.

He was an Assistant professor of electrical engineering with ISEM, Casablanca. Since 2001, he has been a Full Professor with the Faculty of Sciences and Technologies, Cadi Ayyad University, Marrakesh, Morocco. He is a Professor of higher education. He is also the Co-Founder of several training courses with the Faculty of Sciences and Technologies, the Deputy Director of the Electrical Systems, Energy Efficiency and Telecommunications Laboratory, and the Deputy Member of the Management Committee of the Innovation City, Cadi Ayyad University. His research interests include the design, control, modeling, and simulation of energy converters. He is a member of several scientific, reading, and congress organization committees.

SYED UMAID ALI received the B.Eng. degree in electronics from the National University of Science and Technology (NUST), Islamabad, Pakistan, the master's degree from International Islamic University Islamabad, Pakistan, and the Ph.D. degree from the Department of Electrical Engineering, Bahria School of Engineering and Applied Sciences, Islamabad Campus (BSEAS-IC), Pakistan. His research interests include the control of microgrids, fuzzy controllers, model predictive controllers, and hybrid microgrids.

SAEED MIAN QAISAR received the M.S. and Ph.D. degrees in electrical and computer engineering from the Institute National Polytechnic (INP) of Grenoble, Grenoble Alpes University, France, in 2005 and 2009, respectively.

He held a postdoctoral position with the Institute National Polytechnic (INP) of Bordeaux, France. He held different research and development positions in France. He was an Associate Professor and a Researcher with the Electrical and Computer Engineering Department, Effat University, Saudi Arabia. Currently, he is a Research Director with LINEACT CESI, France. He has more than 200 research publications and two patents to his credit and is on the technical review committee of several international conferences and journals. His current research interests include signal processing, circuits and systems, artificial intelligence, event-driven systems, biomedical, smart grid, energy storage, and sampling theory. He is also serving as an editor for international journals.

ASAD WAQAR received the bachelor's degree in electrical engineering from UET Taxila, in 2002, the master's degree in electrical power engineering from RWTH Aachen University, Aachen, Germany, and the Ph.D. degree in electrical power engineering from the Huazhong University of Science and Technology, Wuhan, China, in 2016. He is currently the Director of the post graduate programs with the Bahria University Head Office, Islamabad, Pakistan. He is also a Professor with the Department of Electrical Engineering, Bahria University. Before joining academia, he has vast industrial experience in both locally and internationally. He is actively involved in teaching and research activities. His research interests include smart grids, microgrid operation and control, power quality, power electronics, network reinforcement planning, demand-side management, and big data analysis in power systems. He has successfully supervised more than 50 M.S. and B.E.E. students. He has research publications in many internationally reputed journals and conferences. He has research collaborations with Oregon Tech, USA; Texas A&M University, USA; the Huazhong University of Science and Technology, China; the University of Malaya, Malaysia; King Saud University, Saudi Arabia; and Prince Sultan University, Saudi Arabia. He serves as a Reviewer for IEEE TRANSACTIONS ON POWER SYSTEMS, *Applied Energy*, *International Transactions on Electrical Energy Systems*, IEEE ACCESS, *Renewable and Sustainable Energy Reviews*, and *International Journal for Engineering Science and Technology*.

MOHAMED BAGHDADI received the B.S. degree in industrial informatics and electronics from Mohammed First University, Oujda, Morocco, in 2015, and the M.S. degree in electrical engineering from Cadi Ayyad University, Marrakesh, Morocco, in 2017, where he is currently pursuing the Ph.D. degree in electrical engineering and energy efficiency with the Electrical Systems, Energy Efficiency and Telecommunications Laboratory.

His research interests include semiconductor device models, digital signal processing chips, design, control, modeling and simulation of semiconductor device, and hardware in the loop strategy.

AHMAD ALZAHRANI received the Ph.D. degree from the Missouri University of Science and Technology, Rolla, MO, USA, in 2018. He is currently an Assistant Professor with the Department of Electrical Engineering, Najran University, Najran, Saudi Arabia. His research interests include power electronic converters, renewable energy applications, electric vehicles, energy harvesting, power management, wireless power systems, and power converters design and control.